Realizing up and downlink subcarrier allocation in Orthogonal Frequency Division Duplex (OFDD) Systems*

Shenghong Li and Ross D. Murch
Department of Electronic & Computer Engineering
The Hong Kong University of Science & Technology
E-mail: eelsh@ust.hk, eermurch@ee.ust.hk

***Abstract*—In this paper we describe a new method for multi-carrier systems that allows the allocation of different subcarriers to their up and downlinks. Techniques utilizing such subcarrier allocation have already been used in some cooperation and resource allocation algorithms for multiuser Orthogonal Frequency Division Multiple Access (OFDMA) as well as in Orthogonal Frequency Division Duplexing (OFDD). Therefore it is useful to investigate methods that can enable them. In this work we focus on the physical feasibility of the system since the radio impairments and system imperfections are the key challenges that need to be addressed. In particular we propose a baseband echo cancellation approach to mitigate the interference between the up and downlink subcarriers. An iterative echo canceller is utilized at the receiver, with the reference samples obtained from the output of the transmit power amplifier. The system performance in terms of output signal to interference and noise ratio (SINR) and bit error rate (BER) is evaluated by computer simulations based on the configuration of 802.11a/g systems.**

I. Introduction

As the radio spectrum becomes more and more crowded, efficient use of the spectrum is becoming a major concern in wireless system design, and duplexing is an important factor that needs to be considered. Currently, most communication systems rely on Frequency Division Duplexing (FDD) or Time Division Duplexing (TDD), which assign different frequency bands or time slots for the uplink and downlink. However, either a guard band or guard time is required for these two schemes, leading to a reduction of channel resource utilization. For FDD, the spectrum allocation is fixed and therefore it cannot support flexible allocation of channel resource between uplink and downlink in cases of asymmetric traffic. Moreover, since frequency bands are assigned to FDD systems in pairs, the complexity of spectrum planning is increased.

The concept of subcarrier-based duplexing in OFDM systems has been studied in previous literature [1]–[4]. In this paper, we will follow the terminology in [1] and refer to this technique as Orthogonal Frequency Division Duplexing (OFDD). In OFDD systems, different sets of orthogonal subcarriers are assigned for the uplink and downlink and therefore high flexibility can be achieved in dividing the channel resources by adjusting the number of subcarriers assigned for each direction, which makes it easier to handle asymmetric traffic loads. In addition, through allowing simultaneous transmission and reception on different subcarriers, OFDD makes resource allocation in cooperative multiuser OFDMA networks more feasible [5]–[7].

Subcarrier-based duplexing schemes were first proposed in previous work [3] for digital subscriber line systems. [2] later proposed to interleave subcarriers of an OFDM system for the transmission and reception. Additionally, [1] introduced a scheme where the available subcarriers are allocated in blocks, with an analog filter bank employed to isolate the desired receive signal from transmitting signal and to reduce the signal dynamic range. [4] further considers the time synchronization of OFDD systems, including the time alignment of OFDM symbols and re-establishment of the FFT window. Our contribution is different from the existing work in that we take into consideration RF impairments and system imperfections, which we believe are the most significant issues in realizing a practical OFDD system. The reason for this is that the nonlinear spurious components of the transmitting signal will corrupt the desired received signals since the transmitting signal leaked from the Tx antenna to Rx antenna is much stronger than the received desired signal. A baseband iterative echo canceller is introduced to eliminate this self-interference. The reference signal for performing echo cancellation is obtained from the output of the transmit power amplifier so that the problem of PA nonlinearity and transmitter I/Q imbalance can be circumvented. With such a configuration we believe OFDD can be applied to short range communication systems working in relatively static environments with low transmit power (e.g. 802.11a/g systems).

This paper is organized as follows. In section II, we introduce the basic configuration of OFDD, with the practical limitations described in section III; a detailed description of our system architecture is provided in section IV; simulation results are given in section V and finally a conclusion is provided in section VI.

II. Basic Configuration of OFDD Systems

We consider a basic 802.11a/g system with one base station (BS) and one mobile station (MS). Both stations are transmitting signals to each other simultaneously using the same

*Acknowledge support of Hong Kong Research Grants Council funding HKUST 617508

978-1-4673-0990-5/12/$31.00 ©2012 IEEE

frequency band, but different subcarriers are assigned for the uplink and downlink. For either terminal, the n-th sample of the m-th transmitted OFDM symbol can be written as

$$s(m,n) = \frac{1}{\mathcal{F}} \sum_{k=0,k\in C_{tx}}^{K-1} S(m,k) e^{j2\pi(n-G)k/\mathcal{F}} \quad (1)$$

where $\mathcal{F}$ represents the IFFT/FFT points, G is the length of the Cyclic Prefix (CP) in samples, K is the total number of subcarriers, the index of the samples is $n = 0, 1, ..., G+\mathcal{F}-1$ and $S(m,k)$ denotes the transmit symbol on the k-the subcarrier of m-th OFDM symbol. C_{tx} is the set of subcarriers that is assigned for transmission. Correspondingly, the set of subcarriers for reception is denoted as C_{rx}. C_{tx} and C_{rx} are mutually exclusive, and the union of them represents all the K subcarriers. $s(m,n)$ are concatenated together and fed into a Digital-Analog (DA) converter, resulting in the baseband transmit signal $x(t)$, which is subsequently up-converted and amplified for transmission. In the ideal case, the signal received by the receiver can be expressed as

$$r(t) = x(t) * h(t) + y(t) * g(t) + n(t) \quad (2)$$

where the asterisk denotes the operation of convolution. The first two terms in (2) represent the received near-end signal (self-interference) and far-end signal (desired signal), respectively. $y(t)$ denotes the signal transmitted from the other terminal and $n(t)$ is the received noise. $h(t)$ and $g(t)$ are the channel response for near-end and far-end signal, respectively. After stripping off the CP and applying FFT, the received signal in frequency domain would be

$$R(m,k) = \begin{cases} H_{m,k} S(m,k) + N_{m,k} & k \in C_{tx} \\ G_{m,k} D(m,k) + N_{m,k} & k \in C_{rx} \end{cases} \quad (3)$$

where $H_{m,k}$ and $G_{m,k}$ are the frequency domain response of the near-end channel and far-end channel respectively, k and m are indices of subcarriers and OFDM symbols, respectively. Thus, in the ideal case, orthogonality can be achieved between different subcarriers and between the uplink and downlink. To accomplish this, the received near-end and far-end signals need to be synchronized in time so that a proper FFT window can be established, which is studied specifically in [4].

III. Practical Limitations

In practical systems, perfect orthogonality cannot be guaranteed due to RF impairments and system imperfections. Therefore the following factors need to be considered:

- Dynamic Range of Analog/Digital converter (ADC)
- Nonlinearity of Power Amplifier (PA)
- Phase Noise of Local Oscillator (LO)
- I/Q imbalance
- Carrier Frequency Offset(CFO) of far-end signal
- Time Jitter of ADC/DAC
- Time Synchronization

The problem of Analog-to-Digital converter (ADC) dynamic range arises because the received near-end signal is much stronger than far-end signal. Therefore ADCs with a sufficiently high resolution are required in order to recover the far-end signal successfully. Due to the PA nonlinearity and LO phase noise, the received signal consists of nonlinear spurious signal components of the near-end signal, which will leak into the subcarriers assigned for reception. Although the power of these components is relatively small compared with the linear components of near-end signal, it is still high compared with the far-end signal and therefore the detection of the far-end signal will be severely affected. The I/Q imbalance will generate a 'mirror image' of the transmitting signal and cause interference to other subcarriers [8]. The CFO of far-end signal will also lead to Inter-channel interference (ICI) and Time Jitter of ADC/DAC will limit the achievable SNR. In addition, as has been stated in section II, time synchronization of the received near-end and far-end OFDM symbols is also important so as to facilitate proper re-establishment of FFT window. To overcome these issues, we have proposed a transceiver structure as described in the following section.

IV. System Architecture

The structure of our proposed transceiver is shown in Fig. 1. For simplicity of illustration, it is denoted in baseband equivalent form. The output samples of the OFDM modulator are passed through a pulse shaping filter with an oversampling factor of before being transformed into analog signal. The block denoted 'I/Q error' in Fig. 1 represents the effect of I/Q imbalance introduced during up-conversion. At the receiver

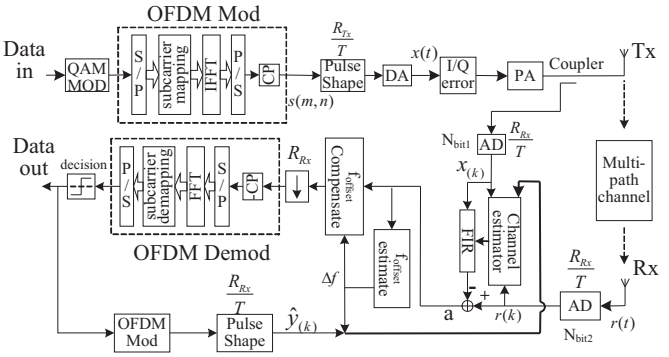

Fig. 1. Structure of proposed OFDD transceiver

side, baseband echo cancellation is employed to suppress the interference on the far-end signal caused by the near-end transmitting signal. The PA output is used as a reference signal for echo cancellation ($x(k)$ in Fig. 1). A coupler is attached to the transmit antenna for this purpose. The key advantage of this approach is that $x(k)$ is a relatively precise representative of the transmitted near-end signal with the effects of transmitting I/Q imbalance and PA nonlinearity included. Therefore the nonlinear spurious components of the near-end signal generated by the nonlinear effect of PA, which is the essential factor that causes interference to the signal on receiving subcarriers, can be suppressed. It is assumed that a one-stage down-converter and digital I/Q demodulation

is employed in the receiver as in [9], and therefore the received signal and reference signal are free of demodulation error during down-conversion. Furthermore, we assume that around 40dB isolation can be achieved between the transmit and receive antennas (this approximately corresponds to 1m separation between the antennas at 2.4GHz; the antennas presented in [10] can also be used, which can provide isolation of higher than 40dB for a bandwidth of up to 20MHz). For short range wireless communication systems with low transmission power (e.g. IEEE 802.11 systems), the maximum allowable transmit power is on the order of 20dBm. In order for the quantization error of the received near-end signal to be lower than the noise floor (such that quantization error will not limit system performance), a 14bit ADC is required, which is high but within current practical implementation limits. What is more, since the transmit signal from the power amplifier is no longer strictly band-limited, baud rate sampling is not sufficient to represent it, and the sampling frequency of the received signal and reference signal needs to be sufficiently high. In this paper, we choose the sampling frequency to be an integral multiple of the baud rate, i.e. $\frac{R_{Rx}}{T}$ as in Fig. 1, with R_{Rx}=4. The cancellation of the near-end signal is carried out on a frame basis. The impulse response of the near-end channel is identified, with which replicas of the near-end signal are generated and subtracted out from the received samples. The cancellation procedure is made up of 2 stages as follows. In the first stage, the channel is estimated based on the whole frame of near-end reference samples $x(k)$ and received samples $r(k)$. We define $\mathbf{r} = [r_{(0)}, r_{(1)}, r_{(2)} \cdots \ r_{(N_f-1)}]^T$ as the received samples, where N_f is number of samples contained in one frame. $\mathbf{r}$ can be approximately written as

$$\mathbf{r} \approx \mathbf{X}\mathbf{h} + e^{j\omega_0}\mathbf{F}\mathbf{Y}\mathbf{g} + \mathbf{z} \tag{4}$$

where $\mathbf{h} = [h_{(0)}, h_{(1)}, h_{(2)} \ldots h_{(L-1)}]^T$ and $\mathbf{g} = [g_{(0)},\ g_{(1)},\ g_{(2)} \ \cdots \ g_{(L-1)}]^T$ denote the Channel Impulse Response of the near-end and far-end channel respectively and L is the order of FIR filters. $\mathbf{X}$ and $\mathbf{Y}$ are defined by

$$\mathbf{X} = [\mathbf{x}_0, \mathbf{x}_1, \ldots \mathbf{x}_{L-1}], \mathbf{Y} = [\mathbf{y}_0, \mathbf{y}_1, \ldots \mathbf{y}_{L-1}] \tag{5}$$

where $\mathbf{x}_i = [x_{(-i)}, x_{(-i+1)}, \ldots x_{(-i+N_f-1)}]^T$, $\mathbf{y}_i = [y_{(-i)},\ y_{(-i+1)},\ \ldots y_{(-i+N_f-1)}]^T$, $i = 0, 1, \ldots L-1$. $x(k)$ and $y(k)$ are near-end and far-end transmit signal, respectively, and $x(k)$ is obtained from the transmit antenna as has been stated. To model the frequency offset of far-end signal,

$$\mathbf{F} = diag([1, e^{j2\pi\omega}, e^{j2\pi\omega\times 2}, \ldots\ldots e^{j2\pi\omega\times(N_f-1)}]) \tag{6}$$

is incorporated in (4), where $\omega = (\Delta f T)/R_{Rx}$. Δf is the carrier frequency difference between near-end and far-end user, while the term $e^{j\omega_0}$ in (4) denotes the initial phase error.

An estimate of the near-end channel impulse response is obtained by the LS algorithm, i.e. $\hat{\mathbf{h}} = \left(\mathbf{X}^H\mathbf{X}\right)^{-1}\mathbf{X}^H\mathbf{r}$ and an estimate of the near-end signal can be generated by $\mathbf{X}\hat{\mathbf{h}}$ and used for echo cancellation. Due to the existence of the far-end signal, which acts as interference in channel estimation, the near-end channel identification is not precise enough and thus the suppression ratio of the near-end signal is not sufficiently high. However, the output far-end signal to residual near-end signal and noise ratio (SINR) is high enough to support the detection of far-end data with a mild error rate. Therefore the frequency offset of the far-end signal can be estimated and compensated, and a hard decision of the far-end message can be determined.

In the second stage, the far-end message detected in the first stage is re-modulated and an estimate of the far-end transmit signal $\hat{y}_{(k)}$ is then constructed by the pre-known pulse shaping filter. This signal, although different from the actual transmit far-end signal due to detection/estimation error and the preclusion of far-end PA nonlinearity and Tx I/Q imbalance, is fed back together with the frequency offset for a more precise identification of the near-end channel. We define $\widehat{\mathbf{Y}}$ and $\widehat{\mathbf{F}}$, which have the structure as (5) and (6) respectively, and are constructed based on the detection result of far-end data. The elements of $\widehat{\mathbf{Y}}$ are $\hat{y}_{(k)}$. The near-end channel impulse response can then be estimated as follows

$$\begin{bmatrix} \hat{\mathbf{h}} \\ e^{j\omega_0}\mathbf{g} \end{bmatrix} = \left(\mathbf{A}^H\mathbf{A}\right)^{-1}\mathbf{A}^H\mathbf{r} \tag{7}$$

where $\mathbf{A}$ is defined as $\mathbf{A} = [\mathbf{X} \quad \widehat{\mathbf{F}}\widehat{\mathbf{Y}}]$. Thus a finer near-end signal cancellation can be carried out. The far-end signal is detected again and used for a new round of near-end channel identification and echo cancellation. This procedure is repeated until a satisfactory suppression ratio and output SINR is obtained. In this work we find that 2 iterations are adequate since the system performance is mainly limited by RF impairments and system imperfection instead of the performance of the mathematical algorithm, especially since the LO phase noise and time jitter of ADC/DAC are difficult to compensate or circumvent. Also taking the time synchronization [4] and channel variation within one frame into consideration, we note that OFDD is more suitable for short-range communication systems working in relatively static environments with low transmit power, and some simulation results will be provided in the following section.

V. Simulation Results

We target a system with parameters similar to those specified by the IEEE 802.11a/g standard. The transmit messages are modulated by QPSK before being passed to the OFDM modulator. No convolution coding or data scrambling is involved in the simulation. The FFT size and CP (Cyclic Prefix) length are 64 and 16, respectively. And the total number of subcarriers is 52. The pulse shaping filter complies with the IEEE 802.11 standard, i.e. Hanning windowed sinc function, with oversampling factor R_{Tx}=16. The I/Q imbalance introduced in the up-conversion is assumed to exhibit an amplitude difference of 1dB and phase difference of 10 degrees between I branch and Q branch, and the power amplifier model in [11] is used to model the effect of PA nonlinearity. Both the near-end and far-end channels are modeled as multipath Rayleigh fading, with the power delay profile (PDP) given by Model D of standard IEEE 802.11 WLAN channel model in [12]. Each

path has a bell Doppler spectrum shape with the maximum Doppler shift set to 6Hz. The carrier frequency offset between the near-end and far-end transmitter is set to 10 KHz. In order to incorporate the effect of LO phase noise, the received samples $r(k)$ in Fig. 1 are processed by $r(k) = e^{j\phi(k)}r(k)$ where $\phi(k)$ has a power spectrum density (PSD) similar to Fig. 4 of [8], except that n1=-110dBc/Hz, which is taken from the datasheet of one state of the art LO as in [13], and n2=-154dBc/Hz. As has been stated in section IV, the isolation between transmit and receive antennas is assumed to be 40dB. The effect of ADCs and DACs is modeled by uniform quantization, and their resolution is chosen to be 14bits. The oversampling factor R_{Rx} at the receiver side is selected as 4, and the echo cancellers use FIR filters with 40 taps. 2 iterations are performed in the 2nd stage echo cancellation. The frame length is chosen to be N_f=3840 and corresponds to a duration of 12 OFDM symbols, noting that a long frame will degrade system performance due to channel variation and LO phase noise, while small N_f will reduce the efficiency of processing. The far-end channel state information are acquired from training symbols and we assume perfect CFO estimation. In addition, the near-end and far-end OFDM symbols are assumed to be aligned in time, such that proper FFT window can be re-established. More sophisticated solutions for time synchronization can be found in [4].

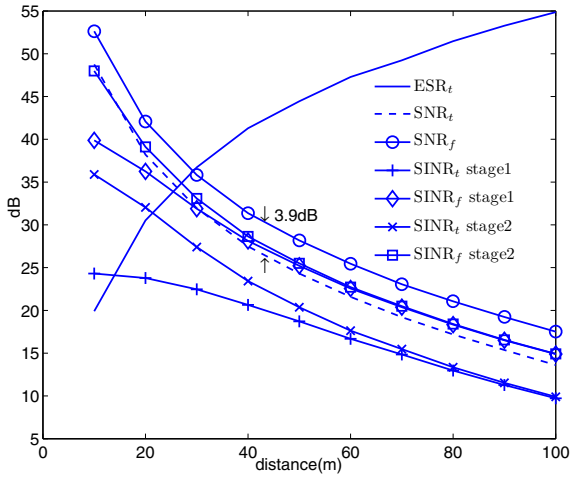

Fig. 2. ESR, SNR and SINR v.s. l with random SC allocation

We use ESR$_t$, SNR$_t$ and SINR$_t$ to represent the received near-end signal to far-end signal power ratio, far-end signal to noise ratio, and output far-end signal to residual near-end signal and noise ratio after echo cancellation (corresponding to point 'a' in Fig. 1), respectively. SNR$_f$ denotes the received far-end signal to noise ratio per subcarrier, averaged over the corresponding subcarriers. SINR$_f$ indicates the SINR per subcarrier after echo cancellation (SINR in frequency domain). Because the power of the transmit signal is spread over 26 subcarriers, while the noise occupies the whole 20MHz bandwidth (64 subcarriers), SNR$_f$ is 10log(64/26) =3.9dB higher than SNR$_t$. The values of ESR$_t$, SNR$_t$, SINR$_t$, SNR$_f$ and SINR$_f$ are plotted in Fig. 2 for different distances between the MS and BS (denoted as l and where we assume a path loss model as that in [12]). Half of the 52 subcarriers are randomly selected for transmission, while the others are for reception. We can see that ESR increases while SNR decreases with l, since the received far-end signal power decays as l increases. SNR$_f$ is higher than SNR$_t$ by 3.9dB as expected. Although the output SINR in time domain is not high, a satisfactory output SINR in frequency domain can be achieved. One interesting phenomenon is that SINR$_f$ can only be improved by the introduction of 2nd stage echo cancellation for small ls. When MS and BS are located far apart, the output SINR$_f$ of the 1st and 2nd stage echo cancellation are almost identical. Therefore the 2nd stage echo cancellation is dispensable in this situation.

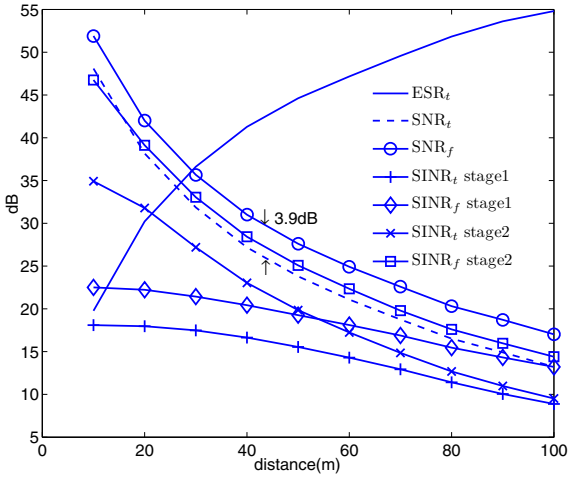

Fig. 3. ESR, SNR and SINR v.s. l with localized SC allocation

Fig. 3 shows the system performance when the first half of the subcarriers are assigned for transmission, while the second half are for reception (localized allocation). It can be seen that the output SINR$_f$ in the first stage is comparatively lower than that in Fig. 2. Therefore unlike the case of random subcarrier allocation, the 2nd stage echo cancellation is necessary here to guarantee a sufficient output SINR. The reason for this phenomenon can be explained as follows. Since the near-end signal and far-end signal occupies different frequency bands, the channel estimation in the 1st stage echo cancellation will place more emphasis on the frequency band of near-end signal, i.e. the frequency response of the obtained near-end channel estimation is accurate in the frequency band of near-end signal but not in the band of far-end signal, therefore the spurious near-end signals generated by PA nonlinearity and phase noise, which spread to the band of the far-end signal, will limit the output SINR. In the case of distributive subcarrier assignment, however, the near-end signal is spread across the whole bandwidth, a more accurate estimation of near-end signal is achievable, thus the near-end signal (including the spurious) is cancelled more accurately. In real applications, the 2nd stage echo cancellation can be activated/disabled

adaptively so as to maximize system performance or reduce complexity, depending on the subcarrier allocation scheme.

In Fig. 4, the achievable total channel capacity of our system is compared with that of single duplex system. The legends in the figure denote the number of subcarriers assigned for uplink (downlink). For example, 13-39 means that 13 out of the 52 subcarriers are randomly allocated for uplink (downlink) while the remaining 39 subcarriers are for downlink(uplink). It can be seen that the total channel capacity is independent of the subcarrier assignment ratio and is almost the same as that of an ideal system where all the available subcarriers are used for transmission in one direction. The results when the antenna isolation is 30dB or 35dB are also included in Fig. 4, with the subcarriers divided evenly between uplink and downlink. We can see that the total channel capacity in this case is lower since the output SINR is decreased due to the increasing of spurious signal power.

Fig. 5 shows the Bit Error Rate (BER) performance of our simulated system with respect to Eb/N0. The theoretical results are also included for comparison. It can be noticed that the BER performance is very close to the theoretical results.

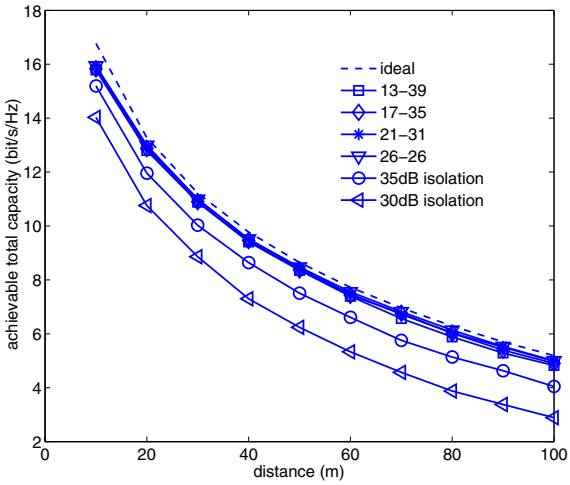

Fig. 4. Total Channel Capacity of OFDD

VI. Conclusion

In this paper, we have proposed a new scheme to achieve OFDD using echo cancellation. We believe that RF impairments and system imperfections are the main factors that limit the performance of OFDD systems and we have therefore devised a system to overcome these issues. A baseband iterative echo canceller based on the output of transmitter PA is proposed to suppress the interference caused by near-end signal on the desired signal. The performance of the OFDD system is evaluated by computer simulation, and it is shown that such a system is feasible by careful design for short-range systems working in a relatively static environment with low transmission power. Future work can focus on the issue of CFO estimation, which is assumed to be prefect in this paper.

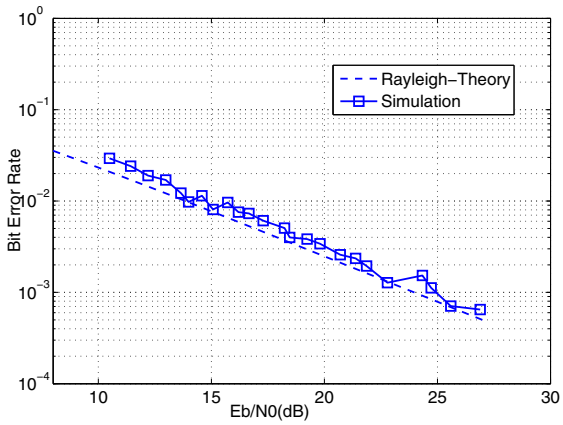

Fig. 5. BER performance of OFDD system

References

[1] R. Kimura and S. Shimamoto, "An Orthogonal Frequency Division Duplex (OFDD) System Using an Analog Filter Bank," *IEEE WCNC 2007*, pp. 2275-2280, Mar. 2007.

[2] D. Steer, K. Teo and B. Kirkland, "Novel method for communications using orthogonal division duplexing of signals (ODD)," *VTC'2002*, vol. 1, pp. 381-385, Sept. 2002.

[3] F. Sjoberg, M. Isaksson, R. Nilsson, P. Odling, S. K. Wilson, and P. O. Borjesson, "Zipper: A Duplex Method for VDSL Based on DMT," *IEEE Trans. Commun.*, vol. 47, Aug. 1999.

[4] C. H. Park, Y. H. Ko, K. W. Park, W. G. Jeon, J. H. Paik, S. P. Lee and Y. S. Cho, "A Synchronous Digital Duplexing Technique for Wireless Transmission in Indoor Environments," *VTC Spring 2009*, pp. 1-5, April, 2009.

[5] L. F. Weng and R. D. Murch, "Cooperation Strategies and Resource Allocations in Multiuser OFDMA Systems," *IEEE Trans. Veh. Technol.*, vol. 58, no. 5, pp. 2331-2342, Jun. 2009.

[6] Z. Han, T. Himsoon, W. P. Siriwongpairat, and K. J. R. Liu, "Resource allocation for multiuser cooperative OFDM networks: Who helps whom and how to cooperate," *IEEE Trans. Veh. Technol.*, vol. 58, no. 5, pp. 2376-2391, Jun. 2009.

[7] G. Li and H. Liu, "Resource allocation for OFDMA relay networks with fairness constraints," *IEEE J. Sel. Areas Commun.*, vol. 24, no. 11, pp. 2061-2069, Nov. 2006.

[8] J. Tubbax, B. Come, L. Van der Perre, S. onnay, M. Engels, H. DeMan, and M. Moonen, "Compensation of IQ imbalance and phase noise in OFDM systems," *IEEE Trans. Wireless Commun.*, vol. 4, no. 3, pp. 872-877, May 2005.

[9] L. Ding, Z. Ma, D. R. Morgan, M. Zierdt, and G. Zhou, "Compensation of frequency-dependent gain/phase imbalance in predistortion linearization systems," *IEEE Trans. Circuits Syst.*, vol. 55, no. 1, pp. 390-397, Feb. 2008.

[10] M. J. Cryan, P. S. Hall, S. H. Tsang and J. Sha, "Integrated active antenna with full duplex operation," *IEEE Trans. Microwave Theory Tech.*, vol. 45, no. 10, pp. 1742-1748, Oct. 1997.

[11] L. Ding, G. T. Zhou, D. R. Morgan, Z. Ma, J. S. Kenney, J. Kim, and C. R. Giardina, "A robust digital baseband predistorter constructed using memory polynomials," *IEEE Trans. Commun.*, vol. 52, no. 1, pp. 159-165, Jan. 2004.

[12] V. Erceg etc, "IEEE P802.11 Wireless LANs," *IEEE 802.11-03/940r4*, May. 2004.

[13] http://www.siversima.com/wp-content/uploads/2009/07/pll_vco20ghz.pdf